



Molecular mechanism for the regulation of human ACC2 through phosphorylation by AMPK

Yong Soon Cho^{a,b,2}, Jae Il Lee^{a,1,2}, Dongkyu Shin^{a,2}, Hyun Tae Kim^a, Ha Yun Jung^c, Tae Gyu Lee^a, Lin-Woo Kang^d, Yeh-Jin Ahn^e, Hyun-Soo Cho^b, Yong-Seok Heo^{c,*}

^a R&D Center, CrystalGenomics, Inc., Seoul 138-739, Republic of Korea

^b Department of Biology, College of Life Science and Biotechnology, Yonsei University, Seoul 120-749, Republic of Korea

^c Department of Chemistry, Konkuk University, Seoul 143-701, Republic of Korea

^d Department of Advanced Technology Fusion, Konkuk University, Seoul 143-701, Republic of Korea

^e Department of Life Science, College of Natural Sciences, Sangmyung University, Seoul 110-743, Republic of Korea

ARTICLE INFO

Article history:

Received 16 October 2009

Available online 10 November 2009

Keywords:

Acetyl-CoA carboxylase (ACC)
Biotin carboxylase (BC)
Fatty acid metabolism
AMP-activated protein kinase (AMPK)
Phosphorylation
Short-term regulation
Soraphen A
Crystal structure

ABSTRACT

Acetyl-CoA carboxylases (ACCs) have been highlighted as therapeutic targets for obesity and diabetes, as they play crucial roles in fatty acid metabolism. ACC activity is regulated through the short-term mechanism of inactivation by reversible phosphorylation. Here, we report the crystal structures of the biotin carboxylase (BC) domain of human ACC2 phosphorylated by AMP-activated protein kinase (AMPK). The phosphorylated Ser222 binds to the putative dimer interface of BC, disrupting polymerization and providing the molecular mechanism of inactivation by AMPK. We also determined the structure of the human BC domain in complex with soraphen A, a macrocyclic polyketide natural product. This structure shows that the compound binds to the binding site of phosphorylated Ser222, implying that its inhibition mechanism is the same as that of phosphorylation by AMPK.

© 2009 Elsevier Inc. All rights reserved.

Introduction

ACC catalyzes the carboxylation of acetyl-CoA to malonyl-CoA. In prokaryotes, ACCs are multi-subunit enzymes consisting of biotin carboxylase (BC), biotin carboxyl carrier protein (bccP), and carboxyl transferase (CT) as separate proteins, whereas eukaryotic ACCs are multi-domain enzymes containing the three domains of each catalytic activity within a single polypeptide chain, in the order BC, bccP, and CT [1].

Mammalian ACC exists as two tissue-specific isozymes: ACC1, present in lipogenic tissues (liver and adipose) and ACC2, present in oxidative tissues (liver, heart, and skeletal muscle) [2]. ACC1 is involved in the biosynthesis of fatty acids, and malonyl-CoA produced by ACC1 is used as a building block to extend the chain length of fatty acids by fatty acid synthase (FAS) [1,3,4]. In contrast, malonyl-CoA produced by ACC2 acts as an inhibitor of carnitine

palmitoyltransferase (CPT I), which is an enzyme that imports fatty acids into the mitochondria for β -oxidation to acetyl-CoA [3].

In mammals, ACC activities of both isoforms are known to be controlled chronically (hours–days) as well as acutely (minutes–hours). The chronic regulation of ACC is carried out through changes in the amount of ACC due to alterations at the level of transcription and mRNA stability, and changes in the rates of enzyme synthesis and degradation [5]. Significant changes in the concentration of ACC do not occur rapidly, since the half-life of ACC in the liver has been reported to be as long as 60 h [6]. Thus, changes in the amount of ACC cannot play a major role in short-term regulation of the enzyme. The acute regulation is achieved via allosteric activation by reversible phosphorylation. ACCs are phosphoproteins and their regulation by reversible phosphorylation is crucial to the control of fatty acid synthesis and oxidation [7]. AMPK (AMP-activated protein kinase) inactivates ACCs by phosphorylating specific serines in the N-terminus *in vivo* [8]. In humans, the major phosphorylation by AMPK occurs at Ser117 of ACC1 and Ser222 of ACC2 [4]. The major role of AMPK in the cell is to monitor its energy status and regulate the ATP-consuming and ATP-producing pathways accordingly. As ACCs catalyze energy-involved pathways of fatty acid synthesis and oxidation by consuming ATP, they are prime physiological targets for AMPK [3]. The active form of mammalian ACCs is a large, linear polymer, with a molecular

* Corresponding author. Address: Department of Chemistry, Konkuk University, 1 Hwayang-dong, Gwangjin-gu, 143-701 Seoul, Republic of Korea. Fax: +82 2 3436 5382.

E-mail address: ysheo@konkuk.ac.kr (Y.-S. Heo).

¹ Present address: Samsung Advanced Institute of Technology, Yongin, Gyeonggi, Republic of Korea.

² These authors contributed equally to this work.

weight of about 8 million Da [1,9]. This polymer is made up of 10–20 protomers, which are dimers of the ACC enzymes [10]. The crystal structure of yeast BC domain in complex with soraphen A, a natural product with potent inhibitory activity against eukaryotic ACCs, showed that the inhibitor binds to the BC dimer interface and inhibits the BC activity allosterically by disrupting polymerization, confirming that polymerization of ACCs is an integral part of its regulation [11,12].

To decipher the molecular mechanism of ACCs inactivation through phosphorylation by AMPK, we determined the crystal structures of human ACC2 BC domain phosphorylated by AMPK, revealing that the phosphorylated Ser222 binds to the dimer interface of BC domain, disrupting the polymerization as soraphen A, whereas the unphosphorylated Ser222 is disordered in the previous structure of the unphosphorylated BC domain [13]. In addition, the crystal structure of human BC domain in complex with soraphen A has been determined, and the structural features of this complex are similar to those of yeast BC domain in complex with soraphen A. This structure could facilitate the discovery of human ACC2 inhibitors for the treatment of obesity and diabetes.

Materials and methods

Protein expression and purification. Both the wild-type and mutants of the human ACC2 BC domain were generated by the standard PCR-based cloning strategy, and their identities were confirmed by sequencing. Residues 217–775 of human acetyl-CoA carboxylase 2 was expressed in BL21 *Escherichia coli* cells at 18 °C using a modified pET21b expression vector encoding additional residues MRGSGS at the N-terminus and LEHHHHHH at the C-terminus. The mutants R277A and E671A were generated by the QuickChange kit (Stratagene) using the expression plasmid of the wild-type as a template. The recombinant proteins were first purified on a nickel agarose (Pharmacia) and then further fractionated by gel-filtration chromatography (Superdex-200, Pharmacia) and anion ion exchange (Mono Q, Pharmacia). In order to phosphorylate the human BC domain, the protein purified as unphosphorylated form was treated with 1.4 unit AMPK (Upstate), 20 mM MgCl₂, 5 mM ATP at 4 °C and further purified with nickel agarose and anion ion exchange.

Crystallization and structure determination. The unphosphorylated and phosphorylated proteins were concentrated to 12 mg/ml in the solution containing 25 mM Hepes (pH 7.5), 150 mM NaCl, 5% Glycerol, and 2 mM DTT. For the crystallization of the human BC domain in complex with soraphen A, the unphosphorylated protein at 12 mg/ml was incubated with 0.1 mM of soraphen A at 4 °C. The phosphorylated BC and the unphosphorylated BC in complex with soraphen A were crystallized in the same condition within a week. The proteins were crystallized at 22 °C by vapor diffusion using hanging-drop method and a protein to reservoir solution ratio of 1:1, with the reservoir solution containing 1.5–1.8 M ammonium sulfate and 0.1 M MES (pH 6.0–6.8). Crystals were transferred to the cryoprotectant solution containing the reservoir solution plus 25% (v/v) glycerol for a few seconds, and then looped from the drop and flash-frozen in liquid nitrogen. The X-ray diffraction data for the crystals were collected at the 4A beam line of Pohang Light Source (PLS). The crystals belong to the spacegroup *P*₃₂₁. The unit cell parameters of the phosphorylated BC crystal are *a* = *b* = 75.7 Å, *c* = 189.5 Å, whereas the soraphen A complex crystal has significantly smaller unit cell dimensions of *a* = *b* = 74.7 Å, *c* = 179.4 Å. Using the program CNS [14], the structure of the phosphorylated BC was solved after one cycle of a rigid body refinement with the structure of the unphosphorylated BC (PDB code 2HJW) as a probe, whereas the structure of the soraphen A complex required a molecular replacement (MR) search due to

the shrink of the unit cell. The structure refinement was carried out with the CNS package and manual model building was performed using the program QUANTA [Accelrys, Inc (San Diego, USA)]. Table 1 summarizes the statistics for data collection and structure refinement. The coordinates and structure factors for the phosphorylated form and the soraphen A complexed form have been deposited in PDB (<http://www.rcsb.org/pdb>) under the accession code of 3JRW and 3JRX, respectively.

Native gel assays. The unphosphorylated form or the phosphorylated form of the wild-type human BC domain, or the mutant proteins were concentrated to 12 mg/ml and incubated with or without 0.05 mM of soraphen A at 4 °C for 1 h prior to electrophoresis. For electrophoresis in a 12% polyacrylamide gel (pH 8.8), 1 µl of the protein solution, and 4 µl of the loading buffer (0.125 M Tris [pH 6.8], 20% [v/v] glycerol, and 0.04% [w/v] bromophenol blue) were loaded for each lane. Electrophoresis was performed in a Tris–glycine running buffer under 70 V at 4 °C for 12 h.

Results and discussion

Structures of the BC domain of phosphorylated form and soraphen A bound form

The crystal structure of the BC domain of human ACC2 of the form phosphorylated by AMPK was determined at 2.6 Å resolution. The overall architecture of the phosphorylated BC domain is the same as that of the unphosphorylated BC domain [13]. The overall structure of human BC domain consists of three domains, the A-domain (residues 217–375), B-domain (residues 436–496), and C-domain (residues 497–775), as well as the AB linker (residues 376–435) that connects the A- and B-domains (Fig. 1A). The putative active site of the human BC domain, where the ATP hydrolysis reaction occurs, is located between the B- and C-domain, despite the absence of ATP in this structure. In the previous structure of unphosphorylated human BC domain, the N-terminus was disordered (residues 217–238), perhaps due to the high flexibility of the loop containing the phosphorylation site including Ser222

Table 1
Statistics on data collection and structure refinement.

	Phosphorylated BC	Unphosphorylated BC/soraphen A
<i>Data collection</i>		
Wavelength (Å)	1.0000	1.0000
Space group	<i>P</i> ₃ ₂ ₁	<i>P</i> ₃ ₂ ₁
Unit cell (<i>a</i> , <i>b</i> , <i>c</i>) (Å)	75.74, 75.74, 189.47	74.74, 74.74, 179.41
Resolution (Å)	2.60	2.50
Observations	95538	183384
Unique reflections	18433	20538
Completeness (%)	91.9 (82.2)	98.9 (98.4)
Average <i>I</i> /σ (<i>I</i>)	29.4 (3.8)	31.5 (4.8)
<i>R</i> _{sym} ^a (%)	6.2 (21.8)	9.8 (39.7)
<i>Structure refinement</i>		
Resolution (Å)	20.0–2.60	30.0–2.50
Reflections (<i> F</i> > 0σ)	18232	19922
<i>R</i> _{cryst} ^b (%)	23.4 (38.6)	22.0 (26.1)
<i>R</i> _{free} ^c (%)	29.4 (42.7)	26.5 (35.1)
R.m.s.d. ^d		
Bonds (Å)	0.008	0.008
Angles (°)	1.3	1.2

Values in parentheses are for the outer resolution shell.

^a *R*_{sym} = $\sum_i \sum_j |I_{h,i} - I_{h,j}| / \sum_i \sum_j I_{h,i}$ for the intensity (*I*) of *i* observations of reflection *h*.

^b *R*_{cryst} = $\sum |F_{obs} - F_{calc}| / \sum |F_{obs}|$, where *F*_{obs} and *F*_{calc} are the observed and calculated structure factors, respectively.

^c *R*_{free} = *R*-factor calculated using 5% of the reflections data chosen randomly and omitted from the start of refinement.

^d Root-mean-square deviations from ideal geometry.

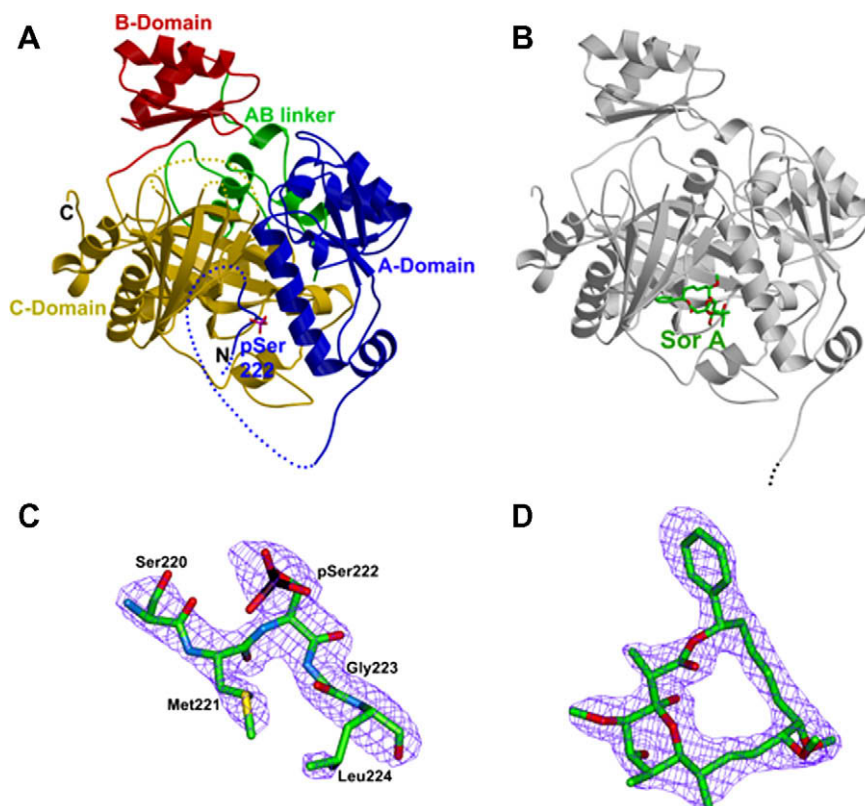


Fig. 1. Overall structure of the BC domain of human ACC2. (A) The phosphorylated BC domain is shown in a ribbon model and the disordered regions (residues 217–219, 225–238, 412–417, 657–665, and 687–698) are expressed as dotted lines. The phosphorylated Ser222 is shown in a stick model of atomic color and labeled pSer222. The four domains are colored differently. The N- and C-terminal regions are also labeled. (B) In the crystal structure of the unphosphorylated BC in complex with soraphen A, the compound is bound to the same site where the phosphorylated Ser222 is bound. Soraphen A is shown in a stick model of atomic color and labeled Sor A. The N-terminal region including Ser222 is disordered in the structure. (C) The sigma-A-weighted $2Fo-Fc$ electron density map calculated with a final refined model of the phosphorylated form without residues 220–224 at a level of 1.2σ . (D) The sigma-A-weighted $2Fo-Fc$ electron density map calculated with a final refined model of the soraphen A complex without soraphen A at a level of 1.2σ .

[13]. What is interesting in the structure of human BC domain phosphorylated by AMPK is that the phosphorylated Ser222 is bound to the soraphen A binding site even though the connecting loop is still disordered (residues 217–219 and 225–238) (Fig. 1A). The electron density for residues 220–224 is clearly shown, and the phosphorylated Ser222 is bound at the interface between the A- and C-domain (Fig. 1C), forming a salt bridge with Arg277 (Fig. 2).

We also determined the structure of unphosphorylated human BC domain in complex with soraphen A at 2.5 Å resolution (Fig. 1B and D). Due to the conservation of the residues involved in binding of soraphen A, the binding mode of soraphen A in human BC domain is substantially the same as that in yeast BC domain [12]. However, upon soraphen A binding to human BC domain, collision causes some conformational changes in Trp681 and Met594 to occur, thereby making a critical contribution to the hydrophobic interaction with soraphen A (Fig. 2). The conformational change of Trp681 is especially drastic upon soraphen A binding to human BC domain, whereas Trp487 of yeast BC domain, which corresponds to Trp681 of human BC, assumes a suitable conformation for recognizing soraphen A prior to binding of soraphen A to yeast BC domain. On the other hand, the phosphorylation of Ser222 does not induce the conformational changes of these two residues as no collision is caused by binding of the phosphorylated Ser222. Arg277 optimizes its conformation to interact with the phosphorylated Ser222 or soraphen A, and its optimum conformation in each structure is supported by the interaction with Glu671, implying the importance of these two residues, Arg277 and Glu671, in

the binding of the phosphorylated Ser222 or soraphen A (Fig. 2). The K_d value of soraphen A for the BC domains of human ACC1 and ACC2 is known to be ~ 1 nM [15]. This high binding affinity of soraphen A is mainly due to the extensive interactions between soraphen A and human BC domain, as in the case of yeast BC domain in complex with soraphen A (Fig. 2C). On the other hand, there is only one interaction between the phosphorylated Ser222 and its binding site: the salt bridge made by Arg277. So, it can be predicted that the inhibitory effect of phosphorylation by AMPK would be much less than that of soraphen A. In other words, this weak binding affinity of the phosphorylated Ser222 could make it possible that the ACC activity *in vivo* is delicately regulated by reversible phosphorylation.

Common inhibition mechanism of phosphorylation by AMPK and soraphen A binding

From the structural information that the phosphorylated Ser222 and soraphen A share a common binding site, we can suggest that phosphorylation by AMPK and soraphen A binding have a common inhibition mechanism (Fig. 3). The bacterial BC subunits are dimeric enzymes, and dimerization is required for their activities [16]. The crystal structures of the bacterial BC subunits show that the dimer interfaces have a twofold symmetry with the dimer axis between the C-domains of each monomers [17]. In our structures, the binding sites of the phosphorylated Ser222 and soraphen A are equivalent to the dimer interface of the bacterial BC subunits. Eukaryotic BC domains are monomeric in solution, and are catalyt-

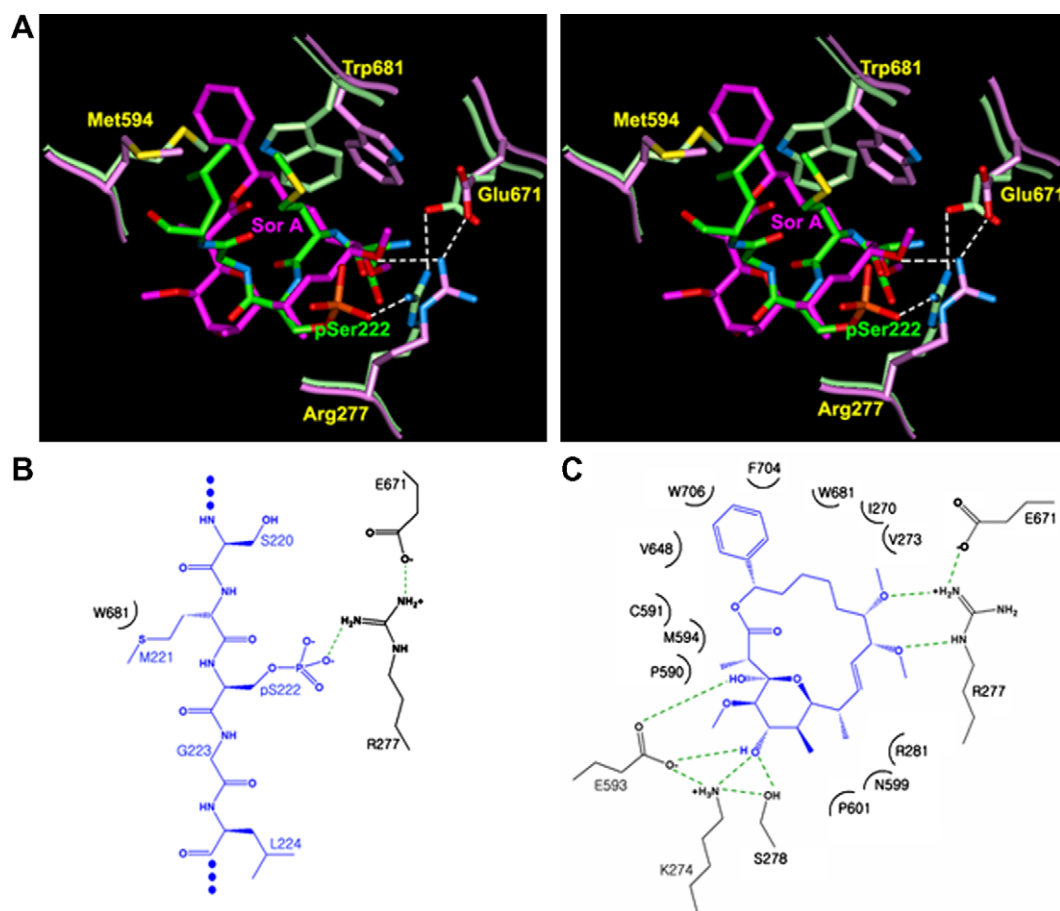


Fig. 2. Interactions of the Phosphorylated Ser222 and Soraphen A in the BC dimer interface. (A) Stereoview of the overlaid dimer interfaces of the phosphorylated form (violet) and soraphen A bound form (green). The phosphorylated Ser222 and soraphen A are labeled pSer222 and Sor A, respectively. The residues with different conformations in the dimer interfaces between the two structures are shown with yellow labels. The hydrogen bonds in the interactions are shown as dashed lines. (B) Schematic representation of the interactions of the Phosphorylated Ser222 in the BC dimer interface. (C) Schematic representation of the interactions of soraphen A in the BC dimer interface. The dashed lines are hydrogen bonds and salt-bridges. The residues involved in hydrophobic interactions are expressed with curves. (For interpretation of the references to colour in this figure legend, the reader is referred to the web version of this article.)

ically inactive [15]. The exact molecular mechanism for the requirement of dimerization for the BC activities is as yet unknown. However, it has been reported that a heterodimer of the *E. coli* BC subunit, in which one monomer has a wild-type active site and the other has an inactivated mutant, has no BC activity, implying the existence of communication between the two active sites [16]. The structural similarity of eukaryotic BC domains to bacterial BC subunits suggests that a similar dimerization may be required for activity of eukaryotic BC domains. Previous studies of yeast BC domain in complex with soraphen A showed that it was likely that soraphen A functions as a protein–protein interaction inhibitor, and abolishes the activity of the BC domain by disrupting its dimerization or oligomerization, thereby leading to the inhibition of the full-length ACC [12]. To investigate the effects of soraphen A on the oligomerization of BC domain of human ACC2, its mobility was examined by a native gel electrophoresis assay. In the absence of soraphen A, the unphosphorylated BC domain of human ACC2 runs as several smeared bands on the gel, whereas in its presence, the protein collapses down to a single band (Fig. 3A). The smeared bands may imply the existence of various states of oligomerization in the absence of the inhibitor. Conversely, the collapsed single band with the fastest migrating speed would correspond to a monomeric state of the BC domain in complex with soraphen A. The same phenomenon has been observed in the native gel assay of the yeast BC domain [12]. From the struc-

tural similarity of soraphen A binding and the same result of the native gel experiment, we conclude that soraphen A likely has a common inhibition mechanism in yeast and human BC domains.

In mammals, the activities of ACCs are subject to acute regulation through phosphorylation by AMPK. The molecular mechanism for the inactivation through phosphorylation by AMPK can be understood from our structure of the phosphorylated BC domain of human ACC2. The active form of mammalian ACC is a large linear polymer. However, if the phosphorylated Ser222 or soraphen A binds to the dimer interface of the BC domain and disrupts the oligomerization of this domain, the active polymer would be degraded to less polymeric forms or a monomer, and its activity thereby decreased. In other words, the unphosphorylated form can be easily activated by polymerization as a result of the uninterrupted dimerization of the BC domain, whereas the phosphorylated or soraphen A bound form would have difficulties in polymerization due to the preoccupation of the BC dimer interface. Observations from the native gel electrophoresis with the phosphorylated BC domain confirm this structural insight. The result from the experiment shows that the phosphorylation of Ser222 by AMPK changes the migration behavior of the BC domain of human ACC2, such that the several smeared bands of the unphosphorylated BC domain collapse down to bands with faster migrating speeds (Fig. 3A). This phenomenon is similar to, but not the same as, the binding of soraphen A. The lower degree of homogeneity of the collapsed bands by

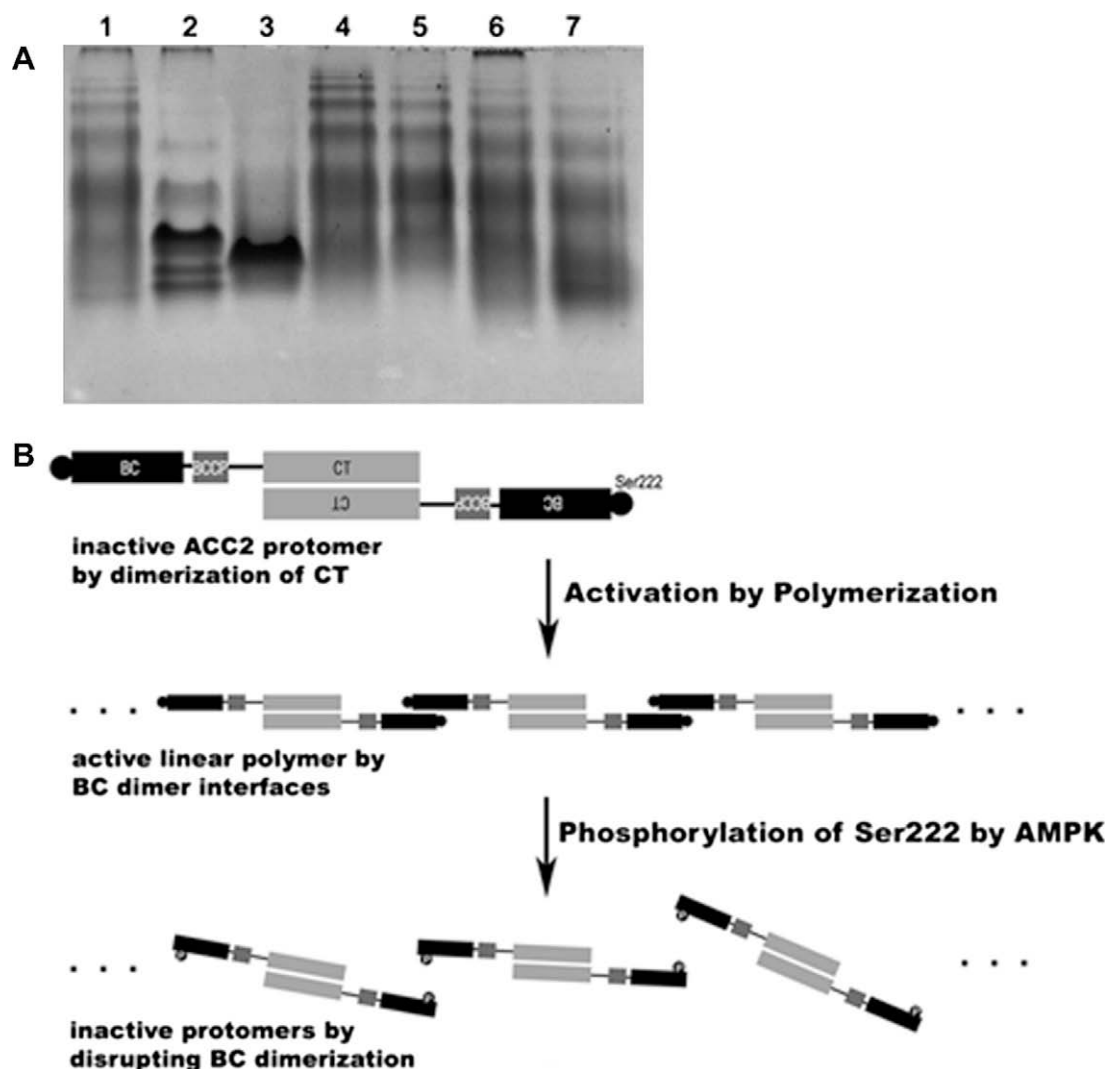


Fig. 3. Proposed mechanism of ACC2 polymerization and inactivation by AMPK. (A) In a native gel electrophoresis with the BC domain of human ACC2, the several smeared bands of the unphosphorylated protein collapsed down as a result of the phosphorylation by AMPK or sorafenib A binding. In mutants R277A and E671A, phosphorylation by AMPK causes little change of the mobility of the proteins from that of the unphosphorylated mutants. *Lane 1*, unphosphorylated wild-type BC domain. *Lane 2*, phosphorylated wild-type BC domain. *Lane 3*, unphosphorylated wild-type BC domain with sorafenib A. *Lane 4*, unphosphorylated R277A mutant. *Lane 5*, phosphorylated R277A mutant. *Lane 6*, unphosphorylated E671A mutant. *Lane 7*, phosphorylated E671A mutant. (B) Schematic drawing of the proposed mechanism of ACC2 polymerization and inactivation. An ACC2 protomer, which is known as a dimer of ACC2, may be generated by the extensive interaction of the CT domains of neighboring ACC2 enzymes in a head-to-tail fashion. When Ser222 is unphosphorylated and unable to bind at the dimer interface of the BC domain, the weak interactions between the dimer interfaces of the neighboring BC domains may enable the protomers to be arranged to make a linear polymer, which is an active form of ACC2. A circle attached to the BC domain shows the location of Ser222. The phosphorylation by AMPK induces the binding of the phosphorylated Ser222 to the dimer interface of the BC domain and inhibits the interactions between the dimer interfaces of the neighboring BC domains, leading to possible degradation of the active linear polymer to inactive protomers. Phosphorylated Ser222 is labeled P inside the circle attached to BC domain.

phosphorylation as compared to the effect of sorafenib A binding may originate from the relatively weaker binding affinity of the phosphorylated Ser222. In the presence of sorafenib A, most BC domains are in a monomeric state due to the tight binding of sorafenib A with a nanomolar K_d value, and so the bands collapse down to a sharp single band corresponding to the monomeric BC domain in complex with sorafenib A. However, phosphorylation by AMPK is likely to shift the equilibrium to less polymeric states of the BC domain, but not leading to exclusive monomerization as sorafenib A does. The importance of Arg277 and Glu671 for the binding of the phosphorylated Ser222 was also evaluated by a native gel electrophoresis (Fig. 3A). In the R277A mutant of BC domain of human ACC2, the migration behavior of the phosphorylated mutant is similar to that of the unphosphorylated mutant R277A without any significant change of the oligomerization state,

implying the salt bridge by Arg277 is of primary importance for binding of the phosphorylated Ser222. In the E671A mutant, some collapse of the bands is observed with a mild change of the polymerization state when the mutant is phosphorylated by AMPK. But the change of the E671A mutant by phosphorylation is not so drastic as that of the wild-type, implying that the role of Glu671 is of secondary importance because it does not interact directly with the phosphorylated Ser222 but facilitates the salt bridge of Arg277 by inducing the optimum conformation of Arg277 for the interaction with the phosphorylated Ser222. The molecular mechanism of the phosphorylation and inactivation of human ACC2 by AMPK can be summarized as the binding of Ser222 phosphorylated by AMPK to the dimer interface of the BC domain, and thereby inhibiting polymerization, which is essential for the activity of the protein.

Proposed mechanism of the ACC polymerization and inactivation by AMPK

From our structural information and the native gel experiments, we can suggest a scenario of the acute ACC regulation including polymerization of ACC and inactivation via phosphorylation by AMPK (Fig. 3B). Polymerization of ACC is the central and most important part of its regulation as the activity of mammalian ACC is absolutely dependent on the state of polymerization. It is known that the active form of mammalian ACCs is a large, linear polymer made up of 10–20 protomers, which are dimers of the ACC enzymes [1,9]. In the crystal structure of the CT domain of yeast ACC, this protein exists as a dimer and the two monomers of the dimer are arranged in a head-to-tail fashion, such that about 5300 Å² of the surface area of each monomer is buried in the dimer interface [18]. Due to this extensive interaction in the dimer interface, the CT domain can exist as a dimer not only in the crystal structure but also in solution. On the other hand, the recombinant BC domain of human ACC2 corresponded to a monomeric state in a gel filtration experiment (data not shown), indicating that the interaction between two BC domains is relatively weak although the protein can belong to several polymeric states at higher local concentration such as the native gel environment. There is 52% sequence identity between the CT domains of yeast ACC and human ACC2, and most of the residues in the dimer interface of the CT domains are highly conserved among eukaryotic ACCs [18]. Therefore, this structural feature of the yeast CT domain should be applicable to the human CT domain. The strong interaction in the dimer interface of the CT domain may serve as a driving force for the generation of ACC protomers, which are dimers of ACC, whereas the weak interaction in the dimer interface of the BC domain would be suitable for the reversible polymerization (Fig. 3B). So, the linear polymer of ACCs as an active form can be constructed by consecutive interactions between the BC domains of the neighboring protomers. When Ser222 is unphosphorylated and unable to bind at the dimer interface of the BC domain, ACC can polymerize easily because the interactions between the BC domains are not interrupted. However, Ser222 phosphorylated by AMPK binds to the dimer interface of the BC domain and interrupts the interaction between BC domains, thereby leading to a breakdown of the linear polymer.

Acknowledgments

We thank the staffs at beamline 4A, Pohang Light Source (PLS), for their assistance. This work was supported by the Korea Research Foundation Grant funded by the Korean Government (MOEHRD). (KRF-2007-313-C00621) and by a Grant (Code #

20070501034003) from BioGreen 21 Program, Rural Development Administration, South Korea. And this work was supported by the Korea Research Foundation grants funded by the Korean Government (KRF-2008-313-C00745 and KRF-2006-005-J04502 to H.S.C.).

References

- [1] S.J. Wakil, J.K. Stoops, V.C. Joshi, Fatty acid synthesis and its regulation, *Annu. Rev. Biochem.* 52 (1983) 537–579.
- [2] L. Tong, Acetyl-coenzyme A carboxylase: crucial metabolic enzyme and attractive target for drug discovery, *Cell. Mol. Life Sci.* 62 (2005) 1784–1803.
- [3] M.R. Munday, D.G. Campbell, D. Carling, D.G. Hardie, Identification by amino acid sequencing of three major regulatory phosphorylation sites on rat acetyl-CoA carboxylase, *Eur. J. Biochem.* 175 (1988) 331–338.
- [4] M.C. Barber, N.T. Price, M.T. Travers, Structure and regulation of acetyl-CoA carboxylase genes of metazoa, *Biochim. Biophys. Acta* 1733 (2005) 1–28.
- [5] M.E. Pape, K.H. Kim, Transcriptional regulation of acetyl coenzyme A carboxylase gene expression by tumor necrosis factor in 30A-5 preadipocytes, *Mol. Cell. Biol.* 9 (1989) 974–982.
- [6] S. Nakanishi, S. Numa, Purification of rat liver acetyl coenzyme A carboxylase and immunochemical studies on its synthesis and degradation, *Eur. J. Biochem.* 16 (1970) 161–173.
- [7] K.H. Kim, F. Lopez-Casillas, D.H. Bai, X. Luo, M.E. Pape, Role of reversible phosphorylation of acetyl-CoA carboxylase in long-chain fatty acid synthesis, *FASEB J.* 3 (1989) 2250–2256.
- [8] D.G. Hardie, D.A. Pan, Regulation of fatty acid synthesis and oxidation by the AMP-activated protein kinase, *Biochem. Soc. Trans.* 30 (2002) 1064–1070.
- [9] J.C. Mackall, M.D. Lane, K.R. Leonard, M. Pendergast, A.K. Kleinschmidt, Subunit size and paracrystal structure of avian liver acetyl-CoA carboxylase, *J. Mol. Biol.* 123 (1978) 595–606.
- [10] F. Ahmad, P.M. Ahmad, L. Pieretti, G.T. Watters, Purification and subunit structure of rat mammary gland acetyl coenzyme A carboxylase, *J. Biol. Chem.* 253 (1978) 1733–1737.
- [11] K. Gerth, S. Pradella, O. Perlova, S. Beyer, R. Muller, Myxobacteria: proficient producers of novel natural products with various biological activities—past and future biotechnological aspects with the focus on the genus *Sorangium*, *J. Biotechnol.* 106 (2003) 233–253.
- [12] Y. Shen, S.L. Volrath, S.C. Weatherly, T.D. Elich, L. Tong, A mechanism for the potent inhibition of eukaryotic acetyl-coenzyme A carboxylase by soraphen A, a macrocyclic polyketide natural product, *Mol. Cell* 16 (2004) 881–891.
- [13] Y.S. Cho, J.I. Lee, D. Shin, H.T. Kim, Y.H. Cheon, C.I. Seo, Y.E. Kim, Y.L. Hyun, Y.S. Lee, K. Sugiyama, S.Y. Park, S. Ro, J.M. Cho, T.G. Lee, Y.S. Heo, Crystal structure of the biotin carboxylase domain of human acetyl-CoA carboxylase 2, *Proteins* 70 (2008) 268–272.
- [14] A.T. Brünger, P.D. Adams, G.M. Clore, W.L. DeLano, P. Gros, R.W. Grosse-Kunstleve, J.-S. Jiang, J. Kuszewski, M. Nilges, N.S. Pannu, et al., Crystallography & NMR System: a new software suite for macromolecular structure determination, *Acta Crystallogr. D Biol. Crystallogr.* 54 (1998) 905–921.
- [15] S.C. Weatherly, S.L. Volrath, T.D. Elich, Expression and characterization of recombinant fungal acetyl-CoA carboxylase and isolation of a soraphen-binding domain, *Biochem. J.* 380 (2004) 105–110.
- [16] K. Janiyani, T. Bordelon, G.L. Waldrop, J.E. Cronan Jr., Function of *Escherichia coli* biotin carboxylase requires catalytic activity of both subunits of the homodimer, *J. Biol. Chem.* 276 (2001) 29864–29870.
- [17] G.L. Waldrop, I. Rayment, H.M. Holden, Three-dimensional structure of the biotin carboxylase subunit of acetyl-CoA carboxylase, *Biochemistry* 33 (1994) 10249–10256.
- [18] H. Zhang, Z. Yang, Y. Shen, L. Tong, Crystal structure of the carboxyltransferase domain of acetyl-coenzyme A carboxylase, *Science* 299 (2003) 2064–2067.